

Optimal power flow management for distributed energy resources with batteries [☆]



Henerica Tazvinga ^{*}, Bing Zhu, Xiaohua Xia

Center of New Energy Systems, Department of Electrical, Electronic and Computer Engineering, University of Pretoria, Pretoria 0002, South Africa

ARTICLE INFO

Article history:

Received 29 September 2014

Accepted 7 January 2015

Available online 29 January 2015

Keywords:

Conflicting

Variable nature

Energy management

Hybrid energy system

Dispatch strategy

ABSTRACT

This paper presents an optimal energy management model of a solar photovoltaic-diesel-battery hybrid power supply system for off-grid applications. The aim is to meet the load demand completely while satisfying the system constraints. The proposed model minimizes fuel and battery wear costs and finds the optimal power flow, taking into account photovoltaic power availability, battery bank state of charge and load power demand. The optimal solutions are compared for cases when the objectives are weighted equally and when a larger weight is assigned to battery wear. A considerable increase in system operational cost is observed in the latter case owing to the increased usage of the diesel generator. The results are important for decision makers, as they depict the optimal decisions considered in the presence of trade-offs between conflicting objectives.

© 2015 Elsevier Ltd. All rights reserved.

1. Introduction

A hybrid renewable energy (RE) system comprising solar photovoltaic (PV) generators, diesel generators (DGs) and battery storage in a hybrid system can solve single source power supply problems. RE systems incorporating DGs and batteries have been studied by various authors, such as Muselli et al. [1], Dufo-Lopez and Bernal-Augustin [2], Jenkins et al. [3], Adaramola et al. [4], but battery wear has not been evaluated in the analyses. The lifetime characteristics of battery energy storage systems have therefore not been fully considered in many RE based hybrid energy management optimization studies. The variable nature of RE sources means that the battery banks in PV applications experience a wide range of operational conditions, including varying rates of charge and discharge, depth of discharge (DoD), temperature fluctuations and charging strategies [5,6]. These operating conditions vary significantly in different locations and applications. Battery lifetime is thus determined by operating conditions, which are a function of the system sizing and the dispatch strategy. In most RE based hybrid systems, battery banks constitute a major part of the investment costs and are often the most expensive component when considering the lifetime costs, as their lifetime is considerably

shorter than that of any of the other hybrid components [7]. Talaq and El-Hawary [5] investigate the performance and expected life-times of different sized batteries, using a previously developed lead acid battery model. The results, based on the lifetime algorithm assumptions used, show that the lifetime of a battery should increase linearly with battery size. Kaiser [8] developed a battery management system that considers the various characteristics of the individual battery strings and decides how the strings are treated considering the load profile. A grid-tied microgeneration and storage model has been developed for quantifying the performance of energy storage options and the challenges of relying on micro-generation for autonomy are highlighted [9]. Riffonneau et al. [10] also propose a grid-tied system with a peak shaving service as a way of increasing the penetration of PV production in the grid and consider battery ageing, but the PV generation is not optimized. An optimal hybrid scheme of a micro-grid with combined heat and power that consists of a gas-engine, wind generator, and PV generator, with the objective of minimizing fuel consumption, is proposed by Hernandez-Aramburo et al. [11]. The bone of contention is that in most optimisation work battery wear cost is neglected, yet battery lifetime in RE based applications poses great uncertainty for investors owing to the replacement cost during the hybrid system's lifetime.

This paper minimizes the operational cost of a PV-diesel-battery (PDB) hybrid system in which lead-acid batteries are used. The main contribution is the consideration of battery wear cost, as battery wear has a great impact on battery life and this has not been considered in the optimization of RE based distributed

[☆] This article is based on a four-page proceedings paper in Energy Procedia Volume 61 (2015). It has been substantially modified and extended, and has been subject to the normal peer review and revision process of the journal.

^{*} Corresponding author. Tel.: +27 12 420 2068.

E-mail address: henerica.tazvinga@up.ac.za (H. Tazvinga).

Nomenclature

$P_1(k)$	control variable representing energy flow from the diesel generator to the load at the k th hour [kW]	$P_{pv}(k)$	the hourly energy output from a PV generator of a given array area at the k th hour [kW h/m ²]
$P_2(k)$	control variable representing energy flow from the PV array and battery at the k th hour [kW]	η_{pv}	the PV generator efficiency
$P_3(k)$	control variable representing energy flow to and from the battery at the k th hour [kW]	E	the battery capacity
$P_L(k)$	control variable representing the load at the k th hour [kW]	η_B	the battery round trip efficiency
A_c	the PV array area [m ²]	$SOC(k)$	the current state of charge of the battery bank

hybrid systems. The model considers hourly fuel and battery wear costs as components of the hybrid system operational cost. The results show the effect of the weighting factors on the system's operational cost and on the state of charge (SOC) of the battery. The effect of restricting the allowable depth of discharge (DoD) is also revealed, as this has a great impact on battery life. The results of this work enable consumers and practitioners to obtain an idea of the system operations and also to appreciate the need for optimal control of the system. Application of multi-objective optimization means that optimal decisions can be achieved in the presence of trade-offs between conflicting objectives. Designers typically arbitrarily assign weight factors either uniformly or based on the significance of the objectives [12,13]. Varying weights and solving each multi-objective problem for its optimum result in various optimal solutions, depending on the weighting factors [14,15]. These solutions are important for designers, performance analyzers, control agents and decision makers who are faced with multiple objectives to make appropriate trade-offs, compromises or choices. Typically, there is an entire curve or surface of points, whose shape depicts the nature of the trade-off between different objectives. In this research, weights could be determined taking into account factors such as energy prices, and environmental concerns. However, in the absence of adequate data concerning such factors, cases with different weights are proposed to determine the overall tendency by considering fuel and battery wear cost while maximizing PV output. It would therefore be convenient to select appropriate weights if corresponding data are available. It is important to note that weight scheduling is still an open question in optimization.

The purpose of the PDB hybrid power system is to supply power to consumers reliably and economically, taking into account fuel and battery wear costs. This work is a follow-up of our previous work that considered only fuel costs, in Tazvinga et al. [22], and also modeling of uncertainties, in Zhu et al. [30]. Modeling of uncertainties is however not included in this paper. This paper is organized as follows: Section 2 describes the problem formulation, Section 3 is the case study and Section 4 covers the results and discussion; the last part is the conclusion.

2. Problem formulation

The PDB system is made up of the PV, DG and battery sub-systems and the configuration is as shown in Fig. 1. The DG supplies the load when the PV output, P_{pv} , the battery output or a combination of the two cannot meet the load. The control variables P_1 and P_2 represent the energy flows from the DG and from the PV generator and battery to the load respectively, while P_3 represents the power flow to and from the battery. Priority is given to the PV generator to supply the load. If the PV output is more than the load, charging power is supplied to the battery. When the PV output is low, the battery supplies power to the load to make up for the imbalance, provided it is within its operating limits. The DG comes

on when the PV and/or battery cannot meet the load. The model is thus able to show the performance of the system in terms of battery dynamics and power flow from each sub-system at any given time interval. The sub-models in the following sub-sections are as described in our previous work [22,24].

2.1. Photovoltaic system model

The hourly power output from the PV generator of a given area is written as:

$$P_{pv} = \eta_{pv} A_c I_{pv}. \quad (1)$$

In Eq. (1), η_{pv} is the efficiency of the PV generator, which can be expressed as a function of the hourly solar irradiation incident on the PV array, I_{pv} (kW h/m²), and the ambient temperature, T_A , as well as the test parameters of the PV generator at standard and nominal cell operating temperature (NT) conditions. A_c is the PV array area and P_{pv} is the hourly power output from a PV generator of a given array area. The efficiency of the PV generator is given by [26]:

$$\eta_{pv} = \eta_R \left[1 - 0.9\beta \left(\frac{I_{pv}}{I_{pv,NT}} \right) (T_{c,NT} - T_{A,NT}) - \beta(T_A - T_R) \right], \quad (2)$$

where η_R is the PV generator efficiency measured at reference cell temperature T_R , i.e., under standard test conditions (25 °C). β is the temperature coefficient for cell efficiency (typically 0.004–0.005 °C); $I_{pv,NT}$ is the average hourly solar irradiation incident on the array at NT (0.8 kW h/m²); $T_{c,NT}$ (typically 45 °C) and $T_{A,NT}$ (20 °C) are, respectively, the cell and ambient temperatures at NT test conditions. The hourly solar irradiation incident on the PV array is a function of time of day, expressed by the hour angle, the day of the year, the tilt and azimuth of the PV array, the location of the PV array site as expressed by the latitude, as well as the hourly global solar irradiation and its diffuse fraction [17–19]. The actual expression relies on the sky model, which is a mathematical representation of the distribution of diffuse radiation over the sky dome presented in Duffie and Beckman [17]. In the study, the simplified isotropic diffuse formula suggested in Collares-Pereira and Rabl [18] is used. The hourly solar irradiation incident on the PV array is given by:

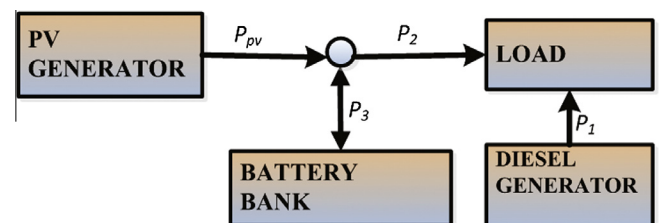


Fig. 1. PDB configuration.

$$I_{pv} = (I_B + I_D)R_B + I_D. \quad (3)$$

In (3), I_B and I_D are respectively the hourly global and diffuse irradiation in kW h/m². R_B is a geometric factor representing the ratio of beam irradiance incident on a tilted plane to that incident on a horizontal plane. Monthly average hourly meteorological data, global irradiation, diffuse irradiation and ambient temperature are used as inputs in evaluating (1)–(3) of the performance simulation model. The evaluation is performed at the mid-point of each hour of the day, on the “average day” of each month as defined in Duffie and Beckman [17]. For any energy supply system, the hourly average energy demand depends on the energy demand profile for the particular application.

A study done at seven South African sites revealed that using monthly average radiation values to model PV performance introduced a mean error of 15.8% when compared to 5-min time step values [31]. Hourly radiation data introduced a much smaller error that can be neglected, justifying why a 1-h step is used in most research works. This time step is used for many solar radiation data sets and is considered adequate for modeling intermittent RE sources with acceptable accuracy, as the underlying principle used to model the system is the same when using a 1- or 5-min and hourly data [32]. The time step used in this work is thus 1 h, as this balances the trade-off among accuracy, computational time, load data and the nature of available RE data for the location considered. Only hourly data are available for the Zimbabwean site under investigation.

2.2. Battery bank model

The power output from the PV and the load demand at a given hour determine the charge or discharge power into and out of the battery bank. k is an integer representing the k th hour interval. The SOC of the battery bank at the next time step, $SOC(k+1)$, depends on the current SOC, $SOC(k)$. At any given hour the battery SOC will be given by the expression:

$$SOC(k+1) = SOC(k) - \alpha P_3(k), \quad (4)$$

in which $\alpha = \eta_B \Delta t / E^{\max}$ and η_B is the battery round trip efficiency, while Δt is the time step. E is the capacity of the battery.

The following general expression applies to the battery dynamics:

$$SOC(k) = SOC(0) - \alpha \sum_{\tau=1}^k P_3(\tau), \quad \text{for } 1 \leq \tau \leq k, \quad (5)$$

where $SOC(0)$ is the initial SOC of the battery.

$P_3(\tau)$ is the charge or discharge rate of the battery at time k .

The available battery bank capacity must not be less than the minimum allowable capacity SOC^{\min} and must not be higher than the maximum allowable capacity SOC^{\max} [8]:

$$SOC^{\min} \leq SOC(k) \leq SOC^{\max},$$

and

$$SOC^{\min} = (1 - DoD)SOC^{\max},$$

where DoD is the depth of discharge expressed as a percentage.

2.3. Battery lifetime modeling

Modeling of the lifetime characteristics of battery energy storage systems is a vital aspect of hybrid power system simulation that has not been fully considered in many RE based hybrid energy management optimization studies [20]. The uncertainty associated with the expected lifetime of the batteries used in RE based hybrid energy systems makes the estimates of cost of energy of the

systems uncertain, as the life cycle cost of the batteries is one of the significant hybrid system expenses.

The two common lead acid batteries lifetime models are the post-processing models and the performance degradation models. The former are pure lifetime models in that they do not include a performance model and can be used to analyze measured data from real systems. The latter integrates a performance model with a lifetime model and the performance model is updated continuously during the simulation so that the performance of the battery can be analyzed depending on the utilization pattern of the battery [21]. There are various methods for calculating the lifetime consumption; these include the Ah-throughput and cycle counting methods. In this work the Ah-throughput counting method is employed to evaluate the lifetime consumption of the battery. This method assumes that a fixed amount of energy can be cycled through a battery before it requires replacement. The estimated throughput, λ_L (the total throughput over a battery bank lifetime), obtained mostly from the DoD vs. cycles to failure curve provided by the manufacturer, is expressed as follows [21]:

$$\lambda_L = DoD_i C_i E, \quad (6)$$

where E is the battery capacity, DoD_i is the DoD being considered, C_i represents the cycles to failure, and i represents each DoD and cycles to failure as given by the manufacturer. Kaiser [8] notes that the degradation of battery bank capacity depends most strongly on the interrelationships of the following parameters: the charging/discharging regime that the battery has experienced, the DoD of the battery over its life, its exposure to prolonged periods of low discharge and the average temperature of the battery over its lifetime. Battery wear is mainly determined by the cycles of the battery, that is, the battery completes a cycle when it is charged and discharged once. In a solar based system, the batteries are charged during the day and discharged at night and this cycle corresponds to one day.

For optimal control formulation, the total throughput of the battery bank over a daily time horizon, λ_D , is given by [29]:

$$\lambda_D = \frac{1}{2} \sum_{k=1}^{24} |P_3(k)|. \quad (7)$$

In order to understand any business model, the cost per cycle, measured in \$/kW h/Cycle, is important. This is obtained by considering the battery cost, which is the sum of the cost of batteries, transportation and installation costs (multiplied by the number of times the battery is replaced during the lifetime of the system). The sum of these costs is divided by the net consumption of the system. The battery bank operating cost over a given day is derived from literature is modeled as [15,27]:

$$B_{op} = \frac{\lambda_D}{\lambda_L} C_b, \quad (8)$$

where B_{op} is the battery operational cost, and C_b is the cost of the battery bank. The battery wear cost, C_{bw} , is expressed as [27]:

$$C_{bw} = \frac{C_b}{\lambda_L}. \quad (9)$$

The battery bank life, B_L , is expressed as [9,27,28]:

$$B_L = \frac{\lambda_{yr}}{\lambda_L}, \quad (10)$$

where λ_{yr} denotes the annual throughput of the battery bank.

2.4. Diesel generator model

DGs are incorporated in hybrid power supply systems as backups. The DG energy dispatch strategy determines the switching on

or off conditions and in this paper, a load-following strategy is employed in which the DG is switched on when the PV and/or the battery is unable to meet the load. In this strategy, the DG is dispatched only when required and this is economical in terms of usage of DG energy and fuel cost. The DG produces only enough power to meet the load demand and does not charge the battery. The DG is more likely to operate at high load factors, resulting in low specific fuel consumption and longer DG life [25]. In this work a variable speed Rush generator type is employed in which an electronic control system is used to vary the output by sensing the load and sending an electrical signal to the fuel injection system to adjust the fuel supply and engine revolutions in response to the load. The advantage of this type of generator is its ability to supply the required power output at any given time [22,16]. The generator is also constrained by its lower and upper operating limits.

3. Case study

The solar radiation data used in this study are calculated from stochastically generated values of hourly global and diffuse irradiation using the simplified tilted-plane model of Collares-Pereira and Rabl [18]. This is calculated for a Zimbabwean site, Harare (latitude 17.80 °S) and the PV data are derived from our previous work [22]. A typical load demand profile for institutional applications that is based on an energy demand survey carried out in rural communities in Zimbabwe is used and the methodology for calculating the load demand profile is as described in Tazvinga and Hove [23]. The load profile is as shown in Fig. 2.

The parameters used in this model are shown in Table 1. The generator cost coefficients are specified by the manufacturer while the DG, PV and battery bank capacities are chosen based on a sizing model developed by Hove and Tazvinga [24]. The system is designed such that demand is met at any given time. A small system means demand will not always be met, while an oversized system means the demand will be met but the system will be unnecessarily costly and energy will be wasted. The sizing is within “rule of thumb” provisions, for example the PV array area for 1 kW p varies from 7 m² to 20 m² depending on cell material used. The energy generated by the PV and the DG is consumed by the load, and the PV and wind generators also charge the battery, depending on the instantaneous magnitude of the load and SOC of the storage battery. The DG on or off times depend on the DG energy dispatch strategy employed. In this work, the load-following strategy is employed whereby the DG switches on when the hourly output of PV is lower than the hourly load and the combined output of the battery and PV cannot meet the load.

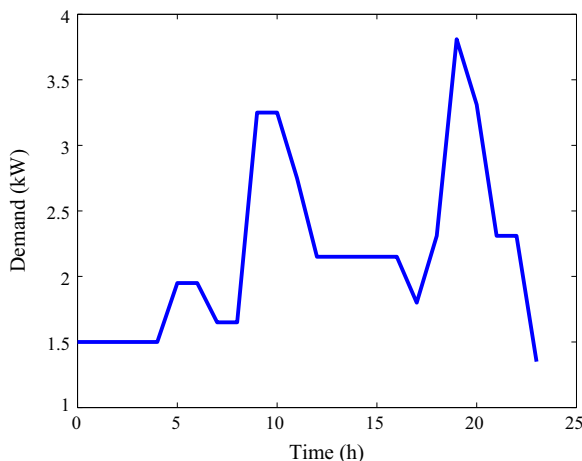


Fig. 2. Typical demand profile.

Table 1
Parameters.

Battery capacity	40 kW h
Battery efficiency	85%
Battery allowable depth of discharge	50%
Battery purchase cost	\$65/kW h
Minimum state of charge	0.5
Maximum state of charge	1
Initial state of charge	0.6
PV array	47 m ²
DG capacity	5 kW A
System voltage	24 V
<i>a</i>	US\$0.246/h
<i>b</i>	US\$0.1/kW h
Fuel cost	US\$1.2/l

3.1. Open loop optimal control model

In order to obtain an optimal operational scheme that balances the objectives in (11), a weighting method is employed to integrate the objectives into one. The sum of the weight coefficients w_1 , w_2 and w_3 is 1 and weight factors indicate the objectives' significance. Each set of weights should generate one optimal solution. Various cases can be considered; however in this paper, two cases are elaborated, when the first two objectives are treated as equally important and when more weight is given to the battery wear cost. This problem is formulated as follows:

$$\min \sum_{k=1}^N (w_1 C_f (aP_1^2(k) + bP_1(k)) + w_2 C_{bw} |P_3(k)| - w_3 P_{pv}(k)) \quad (11)$$

subject to the following constraints:

$$P_1(k) + P_2(k) = P_L(k), \quad (12)$$

$$P_2(k) + P_3(k) \leq P_{pv}(k), \quad (13)$$

$$P_i^{\min} \leq P_i(k) \leq P_i^{\max}, \quad (14)$$

$$0 \leq P_1(k) \leq DG^{\text{rated}}, \quad (15)$$

$$P_3^{\min} \leq P_3(k) \leq P_3^{\max}, \quad (16)$$

$$SOC^{\min} \leq SOC(0) - \alpha \sum_{\tau=1}^k P_3(\tau) \leq SOC^{\max}, \quad (17)$$

for all $k = 1, \dots, N$, where N is 24 and C_f is the fuel price. $w_1 - w_3$ are weight coefficients whose sum is 1. $SOC(0)$ is the initial SOC of the battery. P_i^{\min} and P_i^{\max} are the minimum and maximum limits for each variable. The optimisation problem is solved in a MATLAB environment using the “quadprog” function. This solves problems in the form:

$$\min \frac{1}{2} x^T H x + f^T x,$$

subject to:

$$A x \leq b,$$

$$A_{eq} x = b_{eq},$$

$$lb \leq x \leq ub.$$

4. Results and discussion

Increasing the battery capacity reduces the DoD requirements, thus extending the life cycle of the batteries and reducing interim capital costs, but results in increased initial capital costs. Figs. 3 and 4 show the power flow in case 1: $w_1 = 0.45$, $w_2 = 0.45$, and $w_3 = 0.1$ while in case 2: $w_1 = 0$, $w_2 = 0.9$ and $w_3 = 0.1$ respectively, revealing the effect of different optimal solutions on the operational cost. The power flows in Fig. 3 show that the DG

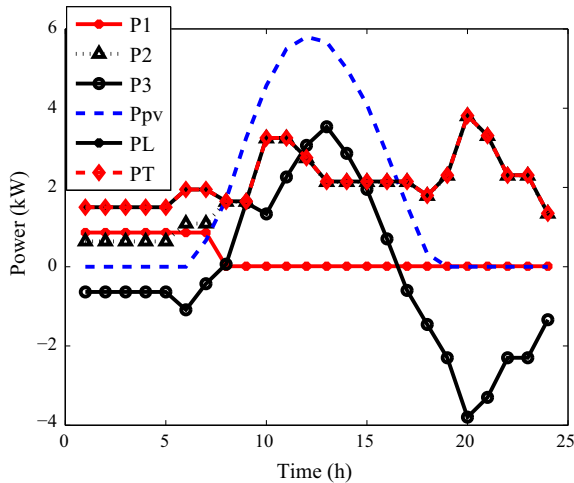


Fig. 3. Optimal power flow for high radiation case 1. Power: from PV = Ppv; DG = P1; to/from battery = P3; to load = P2; load = PL; Power balance = PT.

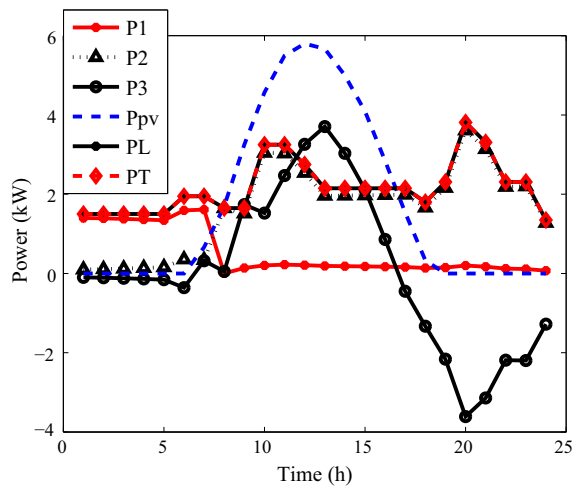


Fig. 4. Optimal power flow for high radiation case 2.

operates only during the early hours of the morning when the SOC of the battery is at such a level that it cannot satisfy the load and the PV is not yet producing any output. During daytime, as soon as the PV can supply the load, the generator switches off completely. The PV system is able to satisfy the load and excess power is used to charge the battery. The total combined power from the PV system and from the battery bank is represented by Graph P2. Graph P2 shows that when the PV system ceases to generate power at the end of the daytime, the battery bank has been charged enough to satisfy the load on its own initially before the DG comes in to cover the imbalance as the battery gets depleted. In Fig. 4 the situation is different, as the DG supplies more power than in Fig. 3 in the early hours of the morning, and also continues to supply reduced power throughout the remainder of the day. The total power supplied to the load, PT, is represented by Graph PT to show the system power balance. Graph PT in both figures shows that the demand is always met completely at any given time, confirming the reliability of the hybrid system.

In Fig. 3, the objectives are treated as equally important, while in Fig. 4 fuel cost is given less weight. When the two cases are compared, there is a considerable increase of 43% in the annual operational cost in favor of the former case. The former case may be considered a more economic dispatch strategy that minimizes

system operation costs. The latter case is an extreme case where fuel cost is given less weight, and the cost increase is due to increased usage of the DG, depicting the importance of balancing and prioritizing the objectives. In the latter case, the DG supplies the load continuously and this may be an unfavorable option for any decision maker, as it results in high DG operation cost and reduces the DG life. The system in this case limits the battery bank usage, resulting in battery life being prolonged at the cost of fuel and DG life. In such a case the DG supplies power during the early morning hours to complement what is coming from the battery. The optimization results thus provide a platform for designers, performance analyzers, control agents and decision makers who are faced with multiple objectives to make appropriate trade-offs, compromises or choices. The results demonstrate that the proposed model can be used to balance the system's operational cost effectively.

While Figs. 3 and 4 show the situation when the radiation output is high, Figs. 5 and 6 show cases where the radiation level is low in the two cases considered above. The major differences in the power flows are the increased usage of the DG to cater for the low power output from the PV system. In all cases shown in the figures the power output from the PV system is maximized. There is still a considerable increase in the operational cost for the weight factors considered. The system's operation costs are also higher than in the case of high radiation owing to the increased fuel cost.

The daily battery operational costs are shown in Fig. 7 for each DoD, showing that the higher the DoD, the higher the battery operation cost. The relationship between battery operational cost and battery wear cost is as given in (8) and (9). It is therefore revealed that the operational cost increases owing to the increase in battery wear as the allowable DoD increases. Fig. 7 shows the fraction of the battery cost used in a 24-h interval. The results show that during system design, it is important to restrict the allowable DoD, as this can improve the cycle life of the battery bank. It is thus shown that the more the battery works, the sooner it will fail, thus higher capacity withdrawal would result in a reduction of battery life cycle.

In Fig. 8 the SOCs of the battery bank are shown for the weighting factors considered in this work. It can be seen that although in all cases the battery bank operates within its limits, for case 1, SOC 1 and case 1, SOC 3, the battery bank is discharged more, while in case 2, SOC 2, and case 2, SOC 4, the battery operates at higher SOCs, as the system penalizes discharging. The less the battery is

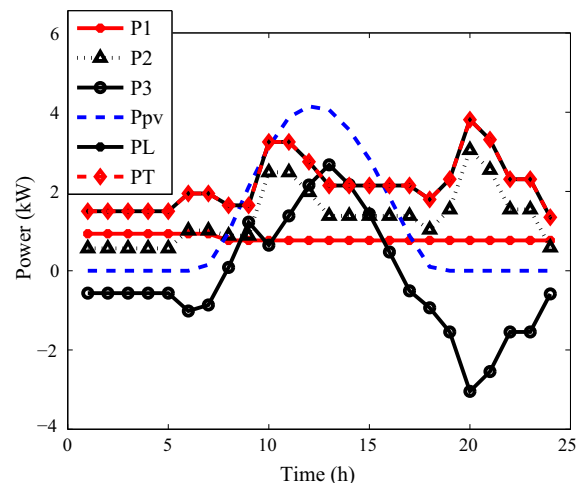


Fig. 5. Optimal power flow for low radiation for case 1. Power: from PV = Ppv; DG = P1; to/from battery = P3; to load = P2; load = PL; Power balance = PT.

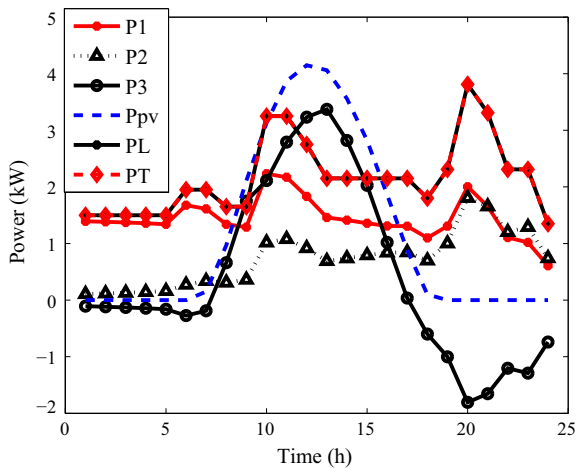


Fig. 6. Optimal power flow for low radiation for case 2.

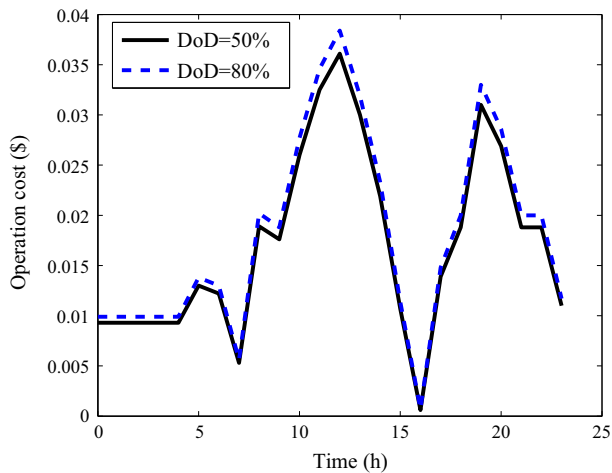


Fig. 7. Comparison of battery wear costs at different DoDs.

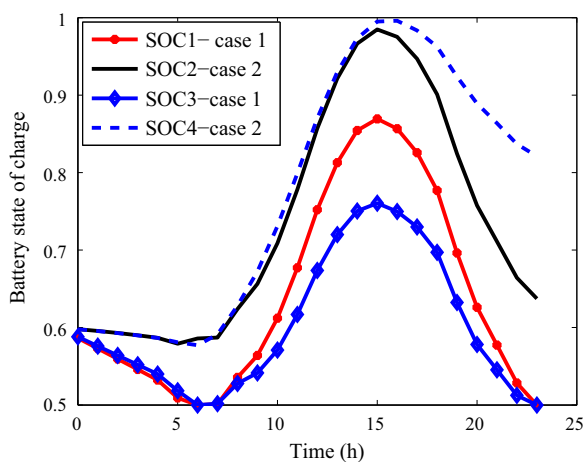


Fig. 8. Comparison of battery states of charge.

discharged, the less the cost per cycle, owing to the fact that if the battery is operated at higher SOC's. The higher the SOC, the less the daily battery throughput, thus the battery bank is preserved more when discharging is penalized. In this work battery life increases, for instance for the high radiation case, from 4.6 years in Case 1

to 9 years in Case 2. It is however important to note that Case 2 is not an ideal case, as it promotes more use of the DG. The results for the cases considered are given to illustrate the effect of limiting battery usage, for instance on fuel cost and on its life span. The results of this work provide a platform for decision makers to make informed decisions by considering various combinations of battery and fuel costs.

5. Conclusion

An optimal model of a PDB hybrid energy management system that minimizes both fuel costs and battery wear costs is presented. Insights into the significance of weight factors are provided and intuition suggests that when a larger weight is assigned to an objective, the optimization result favors that objective. The effect of DoD on battery wear cost has also been shown, confirming that limiting the allowable DoD can prolong battery life in RE based hybrid power supply systems. The optimal model results reveal how the system power flows change in response to the chosen combination of the components of the cost function. A practical platform for decision making has been presented. Future work will include a techno-economic analysis of the system, taking into account various cost combinations. Reduced time steps will also be the subject in our future work for locations that have suitable data, as the current 1 h time step is somewhat coarse. Future work will thus extend the proposed research into continuous cases.

Acknowledgements

The authors acknowledge the support for this work provided by the National Research Foundation of South Africa and the Energy Efficiency and Demand Side Management Hub.

References

- [1] Muselli M, Notton G, Louche A. Design of hybrid-photovoltaic power generator, with optimization of energy management. *Sol Energy* 1999;65(3):143–57.
- [2] Dufo-Lopez R, Bernal-Agustin JL. Design and control strategies of PV-diesel systems using genetic algorithms. *Sol Energy* 2005;79:33–46.
- [3] Jenkins DP, Fletcher J, Kane D. Lifetime prediction and sizing of lead-acid batteries for micro generation storage applications. *IET Renew Power Gener* 2008;2(3):191–200.
- [4] Adaramola MS, Agelin-Chaab M, Paul SS. Analysis of hybrid energy systems for application in southern Ghana. *Energy Convers Manage* 2014;88:284–95.
- [5] Talaq JH, El-Hawary ME. A summary of environmental/economic dispatch algorithms. *IEEE Trans Power Syst* 1994;9(3):1508–16.
- [6] Dagdougui H, Minciardi R, Ouammam A, Robba M, Sacile R. Modeling and optimization of a hybrid system for the energy supply of a “Green” building. *Energy Convers Manage* 2012;64:351–63.
- [7] Svoboda V, Wenzl H, Kaiser R, Jossen A, Baring-Gould I, Manwell J, et al. Operating conditions of batteries in off-grid renewable energy systems. *Sol Energy* 2007;81(11):1409–25.
- [8] Kaiser R. Optimized battery-management system to improve storage lifetime in renewable energy systems. *J Power Sources* 2007;168(1):58–65.
- [9] Jenkins DP, Fletcher J, Kane D. A model for evaluating the impact of battery storage on microgeneration systems in dwellings. *Energy Convers Manage* 2008;49(8):2413–24.
- [10] Riffonneau Y, Bacha S, Barruel F, Ploix S. Optimal power flow management for grid connected PV systems with batteries. *IEEE Trans Sust Energy* 2011;2(3):309–20.
- [11] Hernandez-Aramburo CA, Green TC, Mugniot N. Fuel consumption minimization of a microgrid. *IEEE Trans Ind Appl* 2005;41(3):673–81.
- [12] Dufo-Lopez R, Bernal-Agustin JL, Yusta-Loyo JM, Dominguez-Navarro JA, Ramirez-Rosado JJ, Lujano J, et al. Multi-objective optimization minimizing cost and life cycle emissions of stand-alone PV-wind-diesel systems with batteries storage. *Appl Energy* 2011;88(11):4033–41.
- [13] Liao HL, Wu QH, Li YZ, Jiang L. Economic emission dispatching with variations of wind power and loads using multi-objective optimization by learning automata. *Energy Convers Manage* 2014;87:990–9.
- [14] Konak A, Coit DW, Smith AE. Multi-objective optimization using genetic algorithms: a tutorial. *Reliab Eng Syst Safety* 2006;91(9):992–1007.
- [15] Zhao B, Zhang X, Chen J, Wang C, Guo L. Operation optimization of standalone microgrids considering lifetime characteristics of battery energy storage system. *IEEE Trans Sust Energy* 2013;4(4):934–43.

- [16] Tazvinga H, Zhu B, Xia X. Energy dispatch strategy for a photovoltaic-wind-diesel-battery hybrid power system. *Sol Energy* 2014;108:412–20.
- [17] Duffie JA, Beckman WA. *Solar engineering of thermal processes*. 4th ed. New York: Wiley; 2013. ISBN: 978-0-470-87366-3.
- [18] Collares-Pereira M, Rabl A. Derivation of method for predicting long term average energy delivery of non-concentrating and concentrating solar collectors. *Sol Energy* 1979;22(2):155–70.
- [19] Tiwari GN, Dubey S. *Fundamentals of photovoltaic modules and their applications*. Cambridge: RSC Publishing; 2010. ISBN: 978-1-84973-020-4.
- [20] Achaibou N, Haddadi M, Malek A. Lead acid batteries simulation including experimental validation. *J Power Sources* 2008;185(2):1484–91.
- [21] Binder H, Cronin T, Lundsager P, Manwell JF, Abdulwahid U, Baring-Gould I. Lifetime modelling of lead acid batteries. Technical report. Roskilde, Denmark: Riso National Laboratory; 2005.
- [22] Tazvinga H, Xia X, Zhang J. Minimum cost solution of photovoltaic-diesel-battery hybrid power systems for remote consumers. *Sol Energy* 2013;96:292–9.
- [23] Tazvinga H, Hove T. Photovoltaic/diesel/battery hybrid power supply system: generator component sizing and energy performance analysis. Germany: VDM Publishing; 2010.
- [24] Hove T, Tazvinga H. A techno-economic model for optimising component sizing and energy dispatch strategy for PV-diesel-battery hybrid power systems. *J Energy S Afr* 2012;23(4):18–28.
- [25] Manwell JF, Stein WA, Rogers A, McGowan JG. An investigation of variable speed operation of diesel generators in hybrid energy systems. *Renew Energy* 1992;2(6):563–71.
- [26] Hove T. A method for predicting long-term average performance of photovoltaic systems. *Renew Energy* 2000;21(2):207–29.
- [27] Zhou C, Qian K, Allan M, Zhou W. Modeling of the cost of EV battery wear due to V2G application in power systems. *IEEE Trans Energy Convers* 2011;26(4):1041–50.
- [28] Spiers DJ, Rasinkoski AA. Limits to battery lifetime in photovoltaic applications. *Sol Energy* 1996;58(4):147–54.
- [29] Woon SF, Rehbock V, Setiawan AA. 2008. Modeling a PV-diesel-battery power system: an optimal control approach. In: *Proceedings of the world congress on engineering and computer science*, San Francisco, USA; October 22–24, 2008. p 869–74.
- [30] B Zhu, Tazvinga H, Xia X. Switched model predictive control for energy dispatching of a photovoltaic-diesel-battery hybrid power system. *IEEE Trans Control Syst Technol* 2014;99. <http://dx.doi.org/10.1109/TCST.2014.2361800>.
- [31] Bekker B. Irradiation and PV array energy output, cost, and optimal positioning estimation for South Africa. *J Energy S Afr* 2007;18(2):16–25.
- [32] Madaeni SH, Sioshansi R, Denholm P. Estimating the capacity value of concentrating solar power plants: a case study of the southwestern United States. *IEEE Trans Power Syst* 2012;27:1116–24.